Journal of Statistical Mechanics: Theory and Experiment
An IOP and SISSA journal

Two-scale correlation and energy cascade in three-dimensional turbulent flows

Y X Huang[1], F G Schmitt[2,3,4] and Y Gagne[5]

[1] Shanghai Institute of Applied Mathematics and Mechanics, Shanghai Key Laboratory of Mechanics in Energy Engineering, Shanghai University, Shanghai 200072, People's Republic of China
[2] Université Lille Nord de France, F-59000 Lille, France
[3] USTL, LOG, F-62930 Wimereux, France
[4] CNRS, UMR 8187, F-62930 Wimereux, France
[5] LEGI, CNRS/UJF/INPG, UMR 5519, F-38041 Grenoble, France
E-mail: yongxianghuang@gmail.com, francois.schmitt@univ-lille1.fr and yves.gagne@hmg.inpg.fr

Received 22 October 2013
Accepted for publication 13 March 2014
Published 9 May 2014

Online at stacks.iop.org/JSTAT/2014/P05002
doi:10.1088/1742-5468/2014/05/P05002

Abstract. In this paper, we propose a high-order harmonic-free methodology, namely arbitrary-order Hilbert spectral analysis, to estimate the two-scale correlation (TSC). When applied to fully developed turbulent velocity, we find that the scale-dependent Hilbert energy satisfies a lognormal distribution on both the inertial and dissipation ranges. The maximum probability density function of the logarithm of the Hilbert energy obeys a power law with a scaling exponent $\gamma \simeq 0.33$ in the inertial range. For the measured TSC, we observe a logarithmic correlation law with an experimental exponent $\alpha \simeq 0.37$ on both the inertial and dissipation ranges. The correlation itself is found to be self-similar with respect to the distance between the two considered scales and a central frequency ω_c in the logarithm space. An empirical nonlinear and nonlocal triad-scale interaction formula is proposed to describe the observed TSC. This triadic interaction can be interpreted as experimental evidence of a small-scale nonlinear and nonlocal coupling inside the self-similarity of the Richardson–Kolmogorov phenomenological cascade picture.

1742-5468/14/P05002+15$33.00

Keywords: turbulence

Contents

1. Introduction

In most complex systems, different scales exist simultaneously. They may couple with each other in some linear or nonlinear way. For example, as typical complex systems, turbulent flows are believed to possess different sized eddies [20, 47]. In the framework of the Richardson–Kolmogorov energy cascade picture, the energy is transfered from large to small scales, until the so-called Kolmogorov scale is reached, on which the kinetic energy is converted into heat [20, 47, 43]. It is believed that the different sized eddies interact with each other [35, 15]. Previously, the scale–scale or two-scale correlation (TSC) has been investigated by using a discrete wavelet transform [2, 41, 4, 40] or by using a multiscale correlation [35, 15, 6, 7]. For example, based on discrete wavelet coefficients, Arneodo *et al* [2] proposed a correlation formula for the scale amplitude. However, in the inertial range there is a continuum of eddy sizes and the continuum of scales of the scale correlation should take this into account. On the other hand, a certain scale may not exist all the time [17, 22]. For example, Huang [23] has shown that for several types of data set, the scale is fluctuating and hence has its own distribution; see also the discussion in section 3. Therefore, representation of a time series by using discrete wavelet coefficients may not fully reveal the physical aspect of a real time series [26]. L'vov and Procaccia [35] proposed the so-called fusion rule to identify the interaction between different scales [15, 6]. In their proposal velocity increment is involved, which might mix the information of large-scale and small-scale structures [13, 27, 26]. This might introduce an artificial correlation between different scales. The TSC was also investigated directly in spatial Fourier space by using acoustic scattering measurements based on a Born approximation [5, 44, 11] or by using a sharp Fourier filter bank [1, 14]. We argue here that the Fourier-based methodologies may suffer from a high-order harmonic problem; see the detailed discussion in [26]. The high-order harmonic might lead to an artificial energy redistribution and thus cause an unreal correlation between two different scales [26].

J. Stat. Mech. (2014) P05002

Besides, more and more experimental evidence shows that different sized turbulent structures do interact with each other [36, 8]. For example, in wall-bounded turbulence, Marusic *et al* [36] report experimental evidence of the interaction between large and small scales, in which a so-called very large-scale motion is involved [31, 37]. This finding leads to a new predictable wall-bounded turbulence model [36]. Burger *et al* [8] report a DNS database based visualization of the interaction of the large and small vortices.

To overcome the potential problem mentioned above, we propose in this paper a harmonic-free method, namely arbitrary-order Hilbert spectral analysis [28, 23, 26, 24], to estimate the TSC and to characterize the interaction intensity of two sizes of eddies in a joint physical–spectral domain. The arbitrary-order Hilbert spectral analysis is an extended version of the Hilbert–Huang transform (HHT) [22, 21]. It thus inherits all the advantages of the HHT, such as full adaptiveness and very local ability in both the physical and frequency domains [18]. A nonlinear mechanism, intrawave frequency modulation, is proposed to describe nonlinear processes without involving high-order harmonics [22, 26]; see an example of the nonlinear Duffing equation in [26].

By applying the Hilbert-based method to a fully developed turbulent velocity database, it is found that the Hilbert energy satisfies the lognormal distribution in both the inertial and dissipation ranges. The corresponding logarithm of the Hilbert energy has a power law in the inertial range with a scaling exponent $\gamma = 0.33$. A nonlocal and nonlinear energy cascade is identified by means of an empirical log-law of a two-scale correlation formula with a scaling exponent $\alpha = 0.37$ over a broad range of scales, not only on the dissipation range but also on the inertial range. A triad-scale circle interaction formula, in which the viscosity scale is involved, is proposed to describe the measured TSC. This implies that the fluid viscosity ν (or Kolmogorov scale r_η in the spatial domain or Kolmogorov frequency f_η in the temporal domain) cannot be ignored in the energy cascade process even in the inertial range. The quantitative description of the interaction of the energy cascade presented here is useful for our understanding of the nonlocal and nonlinear energy cascade in hydrodynamic turbulence. The method we propose here is general and applicable to other complex systems.

2. The Hilbert–Huang transform and two-scale correlation

2.1. The Hilbert–Huang transform

We start from the characteristic scales for three different methodologies, i.e., Fourier transform, wavelet transform (Mexican hat) and Hilbert approach. Indeed, the characteristic scale is defined explicitly or implicitly for a given time–frequency analysis method [17, 23]. Figure 1 shows the characteristic scales for Fourier analysis, Mexican hat wavelet and the Hilbert approach we used in this study. They are respectively the length λ of one period of the sine wave, the shape factor a of the chosen mother wavelet together with a scale factor b and the distance between two successive extrema points. Note that the Hilbert approach has a very local definition of the characteristic scale in the physical domain. Once a definition of the characteristic scale has been chosen for a certain method, then the ability and properties of this method are determined/fixed. This is because the conventional idea of time–frequency analysis is

J. Stat. Mech. (2014) P05002

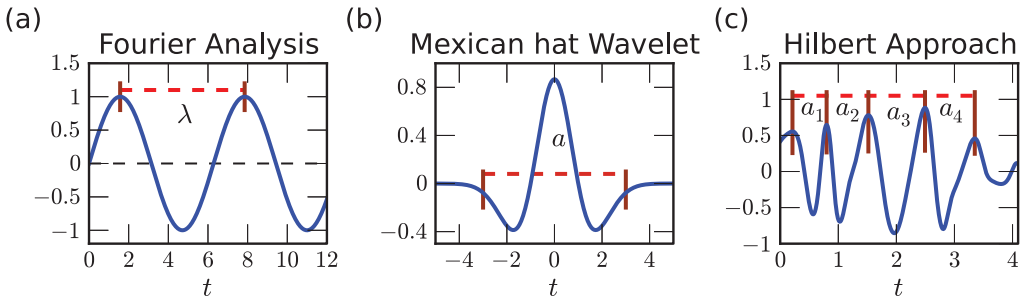

Figure 1. Illustration of the characteristic scale: (a) Fourier transform, (b) wavelet transform (Mexican hat) and (c) the Hilbert-based approach. Note that only the Hilbert methodology allows amplitude and frequency modulation simultaneously, indicating a fully adaptive ability.

to project a given time series to an *a priori* given basis (respectively characteristic scale) [12, 17]. Thus it is an energy-based methodology [17, 22]. However, the Hilbert method extracts the scale information by identifying the local extrema points using the so-called empirical mode decomposition (EMD) algorithm without an *a priori* basis assumption [21, 46, 18]. This is carried out in physical space with a local algorithm [22, 21]. Then, the classical Hilbert spectral analysis, in which a singularity Hilbert transform is involved, is applied to each mode to identify the time–frequency–energy distribution, namely the Hilbert spectrum $H(\omega, t)$, with a very local ability in both the physical and spectral domains [12, 17, 22]. Therefore, the HHT is a scale-based method, in which the basis is deduced from the data themselves.

For a given velocity $u(t)$ measured at a fixed location, the Hilbert methodology first decomposes it into a sum of intrinsic mode functions (IMFs) $C_i(t)$ with a very local ability in the physical domain [22, 21], i.e.,

$$u(t) = \sum_{i}^{N} C_i(t) + r_N(t) \tag{1}$$

in which $r_N(t)$ is a residual. The extracted $C_i(t)$ can be considered as an 'intrinsic' oscillation structure of the turbulence, e.g., a vortex in the statistics sense [45]. Based on the dyadic filter bank property of the EMD methodology, the number N of the IMF mode is limited as

$$N \leq \log_2(L) \tag{2}$$

in which L is the length of the data in points [49, 19, 28, 29]. Then, the Hilbert transform is applied to each IMF $C_i(t)$ to construct the so-called analytical signal, i.e.,

$$\overline{C}_i(t) = \frac{1}{\pi} P \int \frac{C_i(t')}{t - t'} \, \mathrm{d}t', \qquad \tilde{C}_i(t) = C_i(t) + j\overline{C}_i(t) \tag{3}$$

in which P indicates the Cauchy principal value [12, 22, 28]. The amplitude function $\mathcal{A}(t)$ and instantaneous frequency $\omega_i(t)$ are then defined as

$$\mathcal{A}_i(t) = |\tilde{C}_i^2(t)|, \qquad \omega_i(t) = \frac{1}{2\pi} \frac{\mathrm{d}}{\mathrm{d}t} \arctan\left(\frac{\overline{C}_i(t)}{C_i(t)}\right). \tag{4}$$

J. Stat. Mech. (2014) P05002

One can design a joint probability density function (pdf) $p(\omega, \mathcal{A})$ of the $\mathcal{A}$ and ω [28, 27, 26]. The arbitrary-order Hilbert marginal spectrum from $p(\omega, \mathcal{A})$ is then defined as

$$\mathcal{L}_q(\omega) = \int_0^{+\infty} p(\omega, \mathcal{A}) \mathcal{A}^q \, \mathrm{d}\mathcal{A} \tag{5}$$

in which $q \geq 0$ [28, 26]. When $q = 2$, one recovers the so-called Hilbert marginal energy spectrum, which describes the energy distribution against the frequency ω [28, 23]. The method has been successfully applied to turbulent velocity [28], passive scalar [26], Lagrangian turbulence [24], river turbulence [29], vorticity statistics in two-dimensional turbulence [45], etc, to characterize the intermittent nature of these processes [23]. For details on this methodology, we refer to [22, 21, 18, 28, 23, 27, 26].

2.2. Two-scale correlation: definition and validation

We introduce here a second-order Pearson two-scale-correlation formula for the Hilbert energy $E_H(\omega, t) = \mathcal{L}_2(\omega, t)$ (we work in the temporal domain, it does not change the main conclusion of this paper), i.e.,

$$\mathcal{R}(\omega_1, \omega_2) \equiv \frac{\langle (E^H_{\Delta T}(\omega_1, t) - \overline{E^H_{\Delta T}(\omega_1)})(E^H_{\Delta T}(\omega_2, t) - \overline{E^H_{\Delta T}(\omega_2)}) \rangle_t}{\sigma(E^H_{\Delta T}(\omega_1)) \sigma(E^H_{\Delta T}(\omega_2))} \tag{6}$$

in which $\langle \bullet \rangle_t$ is the time ensemble average over the whole time span, $E^H_{\Delta T}(\omega, t)$ is the energy provided by the Hilbert method at scale ω, $\overline{\bullet}$ is the mean value, $\sigma(\bullet)$ is the standard deviation and ΔT is a time span in which $E^H_{\Delta T}(\omega, t)$ is estimated. By definition, we have $\mathcal{R}(\omega_i, \omega_j) = \mathcal{R}(\omega_j, \omega_i)$ and $\mathcal{R}(\omega_i, \omega_j)|_{i=j} = 1$. Equation (6) can be interpreted as a coupling between two different scales. Specifically, for turbulent flows, $\mathcal{R}(\omega_1, \omega_2)$ quantitatively characterizes the interaction intensity (respectively coupling) between two sizes of eddies. Equation (6) has some similarities with structure-function multiscale correlations [35, 15, 6, 7]. Here, we consider it for the first moment and using the Hilbert method. We focus on the frequency dependence.

We provide here some comments on the choice of the time span ΔT. In practice, the choice of ΔT has to be made with caution. A proper size of ΔT should be chosen based on the process itself. Too small a ΔT will introduce a strong bias when calculating $\mathcal{R}$, while too large a ΔT might average out the true correlation information. In our experience, the measured $\mathcal{R}$ is independent of ΔT in a large range of ΔT for both synthesized fractional Brownian motion (fBm) data and experimental data.

We validate here the proposed TSC by using an fBm simulation. fBm is a classical mono-fractal process without any intrinsic structure. Therefore, the corresponding $\mathcal{R}$ is a Dirac Delta function, $\mathcal{R}(\ell_i, \ell_j) = \delta_{i,j}$, in which ℓ_i could be any definition of the scale, e.g., instantaneous frequency ω in Hilbert spectral analysis, the separation r in the structure-function (SF) analysis, the scale l in wavelet transform (WT), etc. We perform 8760 realizations of fBm simulation with 2^{14} data points each by using a Fourier-based Wood–Chan algorithm [48]. We then estimate the Hilbert marginal energy $\mathcal{L}_2(\omega)$, second-order SF $S_2(\tau)$ and the energy of continuous (respectively discrete) wavelet transform (CWT) (respectively DWT) $Z_2(l)$ with the db3 wavelet, respectively with $\Delta T = 2^{14}$ data points.

J. Stat. Mech. (2014) P05002

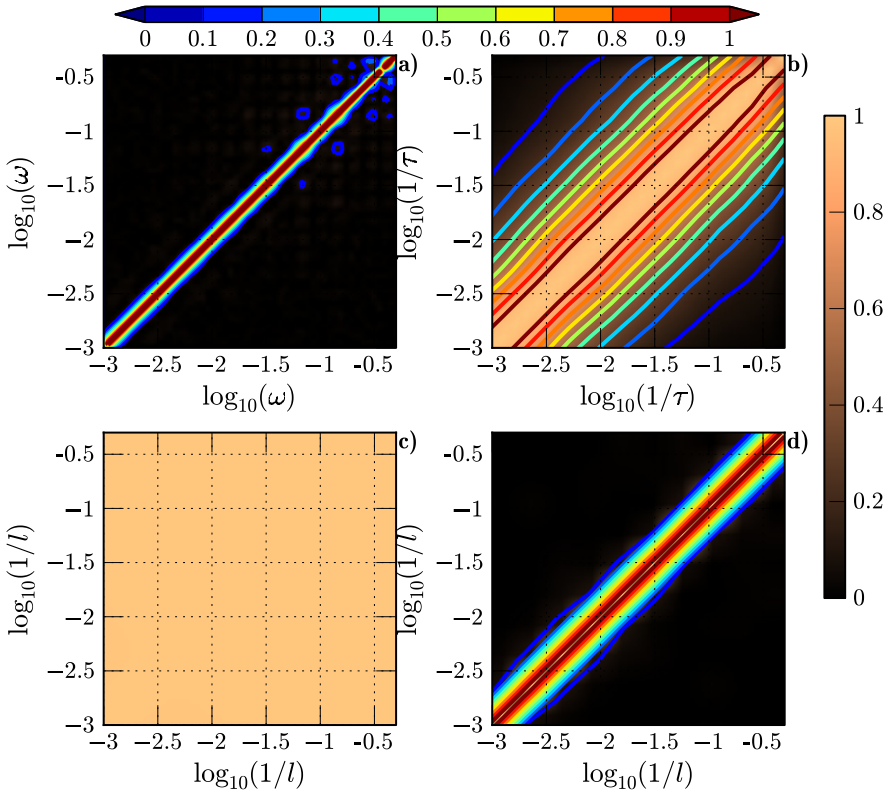

Figure 2. Contour plot of the calculated two-scale correlation $\mathcal{R}$ for a fractional Brownian motion simulation with $H = 1/3$. (a) Hilbert spectral analysis, (b) second-order SF, (c) continuous wavelet transform and (d) discrete wavelet transform with the db3 wavelet. Since there is no intrinsic structure in the synthesized fBm data, a Dirac Delta function $\mathcal{R} = \delta_{i,j}$ is expected. Only the Hilbert-based method predicts the correct $\mathcal{R}$. An explanation for this result is illustrated in figure 3 by using a weight function $\mathcal{W}(f)$ in Fourier-frequency space.

Figure 2 shows the TSC for the above mentioned methods. For convenience of comparison, we convert the results of SF and CWT (respectively DWT) into spectral space by taking $1/\tau$ and $1/l$.[6] Visually, the Hilbert result agrees very well with the statement we made above, i.e., $\mathcal{R}(\omega_i, \omega_j) = \delta_{i,j}$. CWT predicts an artificial correlation $\mathcal{R} \geq 0.99$ for all scales due to a band-pass property of the transform. DWT provides a comparable result to the Hilbert method. As already mentioned above, it provides information only on discrete scales, which is obviously not the case for complex systems.

To further explain the above results, we introduce here a weight function $\mathcal{W}$ to characterize the different scale contributions to the corresponding energy (or the second-order statistical moment) in a Fourier spectral space for a linear and stationary process, i.e.,

$$E(\ell) = \int_0^\infty \mathcal{E}(f)\mathcal{W}(\ell, f)\,\mathrm{d}f \tag{7}$$

[6] One may relate the wavelet scale l with the frequency f more precisely with a definition of the central frequency. However, it does not change the conclusion here.

J. Stat. Mech. (2014) P05002

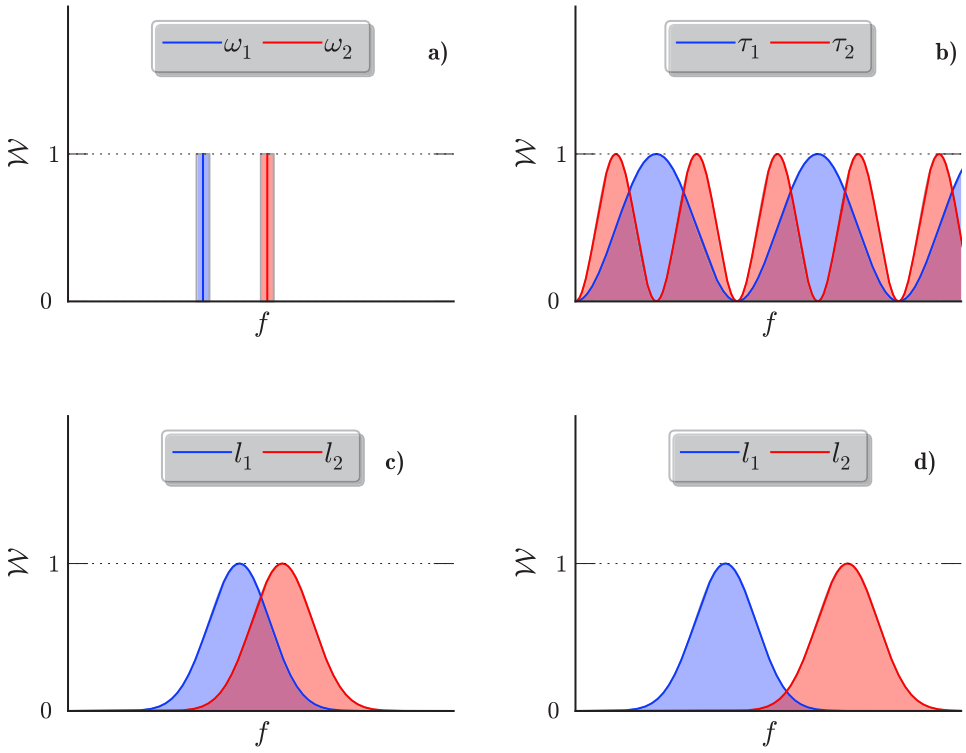

Figure 3. Comparison of the weight function $\mathcal{W}(f)$ of the two scales for different methods in Fourier-frequency space: (a) Hilbert spectral analysis, (b) second-order structure function, which can be obtained by using the Wiener–Khinchin theorem, (c) continuous wavelet and (d) discrete wavelet. For wavelets, the weight function is a band-pass filter. The exact shape of the weight function $\mathcal{W}$ depends on the chosen wavelet family. The overlap range indicates the origin of the artificial correlation.

in which $\mathcal{E}(f)$ is the Fourier power spectrum of the original variable and ℓ is the scale. For nonlinear and nonstationary processes it might only be an approximation. Thus, qualitatively speaking, the analysis presented here holds approximately for all types of stochastic processes. We show in figure 3 the corresponding $\mathcal{W}$ for a linear and stationary process, e.g. fBm. For the Hilbert method, $\mathcal{W}$ is a Dirac function $\delta_{\omega,f}$. For the SF, $\mathcal{W} = 1 - \cos(2\pi f\tau)$, in which τ is the separation scale, obtained by using the Wiener–Khinchin theorem [42, 27]. The CWT and DWT are band-pass filters. Their exact shape depends on the choice of the wavelet family. The overlap range indicates an origin of an artificial TSC, since the same Fourier frequency has contributions at two different scales. In principle, the above argument is only valid for linear and stationary processes. However, it could be approximately valid for nonlinear and nonstationary processes. We recognize that Fourier-based methods require high-order harmonic components to represent nonlinear and nonstationary processes, such as coherent structures, ramp–cliff structures in passive scalar turbulence [27], etc. They might lead to an artificial energy redistribution from large scales (low frequency) to small scales (high frequency) in spectral space and will cause an artificial TSC as well [26].

J. Stat. Mech. (2014) P05002

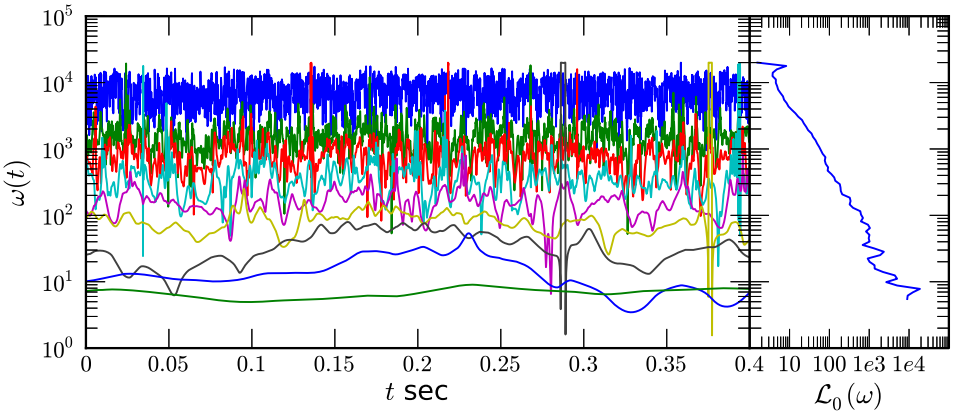

Figure 4. Left: an example of the measured instantaneous frequency $\omega(t)$ for a 0.41 s portion of the longitudinal velocity. Right: the corresponding zeroth-order Hilbert marginal spectrum $\mathcal{L}_0(\omega)$, which is indeed the marginal distribution of instantaneous frequency.

3. Experimental results

We consider here a turbulent velocity database obtained from an experimental homogeneous and nearly isotropic turbulent channel flow, in which an active-grid technique is performed to achieve high Reynolds number. We use the data obtained at downstream $x/M = 20$, where M is the mesh size. At this measurement location, the mean velocity is $\langle u \rangle = 12.0$ m s^{-1}, the turbulence intensity is 15.4% and the Taylor microscale based Reynolds number is $Re_\lambda \simeq 720$. The sampling frequency is 40 kHz and the measurement noise is around $f_\mathrm{N} \simeq 20$ kHz [32]. An inertial range is found in the range $10 < f < 1000$ Hz. The corresponding integral time scale is $T_0 = \ell/u_\mathrm{rms} \simeq 0.14$ s, corresponding to $f_0 \simeq 7.5$ Hz. The Kolmogorov dissipation frequency is about $f_\eta = \tau_\eta^{-1} = (\epsilon/\nu)^{1/2} \simeq 1200$ Hz[7], in which ϵ is the mean energy dissipation rate and ν is the viscosity [43]. Above this frequency the eddy motion is dominated by the viscosity. More details about this database can be found in [32].

In calculating $E_H(\omega, t)$, a suitable time span ΔT should be chosen. We take $\Delta T \simeq 0.41$ s, corresponding to 2^{14} data points. It is about 3.3 times the integral time scale T_0. Thus, at least one complete Richardson–Kolmogorov cascade procedure or one complete eddy for a certain size ω is contained in this time span. If the time span ΔT is too short, $E_H(\omega, t)$ will contain the partial energy of an eddy with size ω. Thus, the $\mathcal{R}$ will be strongly biased. If ΔT is too large, $\mathcal{R}$ will be averaged out since the variation of the Hilbert energy $E_H(\omega, t)$ can be excluded. A test with various values of ΔT with $\Delta T = 2^5 \sim 2^{14}$ data points has been performed. It is found experimentally that when $\Delta T > 2^{12}$ data points the results are not changed. Figure 4 displays an example of the measured instantaneous frequency $\omega(t)$ (left) and the corresponding zeroth-order Hilbert marginal spectrum $\mathcal{L}_0(\omega)$ (right), respectively. Mathematically speaking, $\mathcal{L}_0(\omega)$ is the

[7] The data set has no spatial resolution for the Kolmogorov dissipation scale r_η. The dissipation scale is estimated by an indirect method; see more detail in [32].

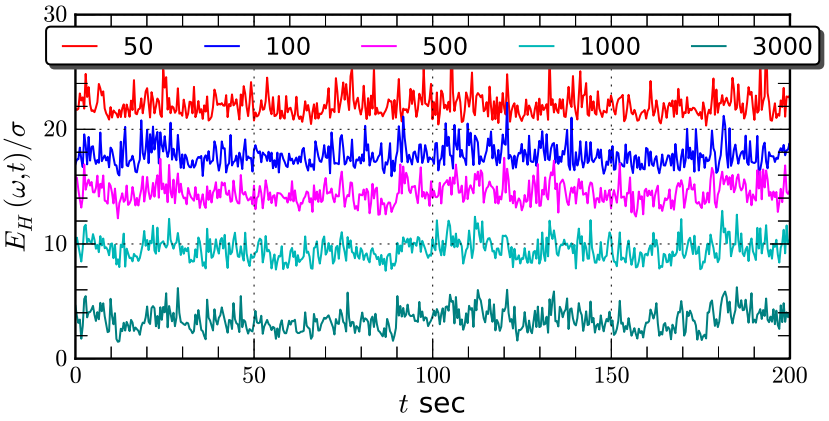

Figure 5. A 200 s portion of the evolution of the Hilbert energy $E_H(\omega,t)/\sigma$ (σ is the standard deviation of $E_H(\omega)$) for longitudinal velocity in a fully developed turbulent flow with a Taylor microscale based Reynolds number $Re_\lambda \simeq 720$ for various scales (from top to bottom) in the inertial range (50, 100, 500 and 1000 Hz) and a dissipation range of 3000 Hz. For clarity of display, the curves have been vertically shifted.

marginal distribution of ω. As mentioned above, the instantaneous frequency ω is indeed discretely distributed in the time–frequency space, and is continuously distributed in a statistical sense [23]. Note that the Hilbert-based method is a fully data-driven method, in which the basis is derived by the data themselves. Therefore, whether the marginal distribution of ω is continuous or not depends on the process itself. Usually, for a stochastic process, the measured $\mathcal{L}_0(\omega)$ is continuous. Figure 5 shows a 200 s portion of the evolution of the normalized Hilbert energy $E_H(\omega,t)/\sigma$ (σ is the standard deviation of $E_H(\omega,t)$) with $\Delta T \simeq 0.41$ s for various scales in the inertial and dissipation ranges. They show similar evolution trends. For example, we observe an energy bump around $20 < t < 30$ s for all five scales, indicating a coupling between these scales. Figure 6 displays the measured probability density function (pdf) of the Hilbert energy $E_H(\omega,t)$ for the same given scales as in figure 5. Note that we take the logarithm of $E_H(\omega)$ and normalize it by its standard deviation $\sigma(\omega)$. For comparison, the normal distribution is also presented as a solid line. Visually, apart from the left tail $X(\omega,t) = \log_{10}(E_H(\omega,t)) < -3\sigma$, the Hilbert energy $E_H(\omega)$ satisfies a lognormal distribution in both the inertial and dissipation ranges. It is interesting to note that a lognormal distribution has been observed for the energy of large-scale fluctuations by using the velocity increment to separate different scales in the physical domain directly [39].

Recently, Huang *et al* [30] discovered a scaling of the maximum pdf of the increment of a scaling time series. Instead of the increment, we apply here the same idea to the logarithm of the Hilbert energy $E_H(\omega)$ without renormalization in the logarithmic frame. We show the maximum pdf, i.e., $p_{\max}(\omega) = \max_{E_H}\{p(X(\omega))\}$, and $X(\omega,t) = \log_{10}(E_H(\omega,t))$, as the inset in figure 6. It is interesting to observe a power law behavior, i.e., $p_{\max}(\omega) \sim \omega^\gamma$, in the range $20 < \omega < 800$ Hz with a scaling exponent 0.33 ± 0.01. This also indicates that the standard deviation σ satisfies a power law relation in the same scale range, i.e.,

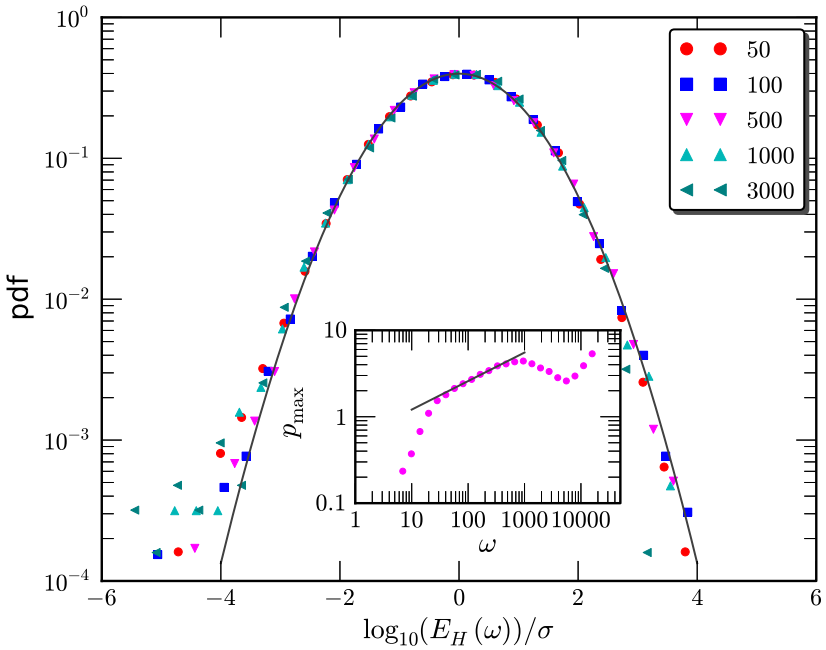

Figure 6. The measured pdf of the Hilbert energy $E_H(\omega, t)$ for the same scales as in figure 5. Note that, apart from the left tail, the Hilbert energy satisfies a lognormal distribution very well. The inset shows the maximum pdf $p_{\max}(\omega) = \max_{E_H}\{p(\log_{10}(E_H(\omega)))\}$. A power law behavior, i.e., $p_{\max}(\omega) \sim \omega^{\gamma}$, is observed in the range $20 < \omega < 800$ Hz with a scaling exponent $\gamma = 0.33 \pm 0.01$. It also indicates a power law relation $\sigma(\omega) \sim \omega^{-\gamma}$.

$\sigma(\omega) \sim \omega^{-\gamma}$, since $X(\omega, t)$ is close to having a lognormal distribution [30]. The observed scaling exponent is occasionally consistent with the Kolmogorov value of 1/3.

Figure 7 shows the contour plot of the measured $\mathcal{R}$ provided by four methods. They are (a) the second-order Hilbert marginal spectrum $\mathcal{L}_2(\omega)$, (b) the second-order SF $S_2(\tau)$, (c) the second-order continuous WT and (d) the discrete WT spectrum $Z_2(\ell)$. The Kolmogorov dissipation frequency f_η is indicated by a horizontal solid line. The measurement noise is detected by the Hilbert methodology above $f \simeq 10$ kHz, which is also confirmed by the Fourier power spectrum [32]. This means that above this frequency, the signal is gradually dominated by the measurement noise. Other methods, such as SF analysis, WTs, etc, fail to detect the measurement noise. One can also find that apart from the Hilbert approach, the rest of the methods provide a higher index value of $\mathcal{R}$ for $f > 10$ kHz. Note that the measured $\mathcal{R}$ are completely different from the one for the fBm with $H = 1/3$, see figure 2. This is because there are indeed 'intrinsic structures' of turbulence present in the turbulent data, demonstrating the physics of turbulence. We then focus on the Hilbert result only below.

Figure 8(a) reproduces the contour plot of the measured TSC $\mathcal{R}$. It is interesting to note that a correlation with $\mathcal{R} \geq 0.8$ starts from f_η and ends at $f \simeq 10\,000$ Hz, which is indicated by arrows. We may consider this range as the dissipation range, in which the flow is dominated by viscosity. Thus, in this range, due to the effect of viscosity, the different sizes of eddies are almost linearly correlated with each other, indicating that the eddy

J. Stat. Mech. (2014) P05002

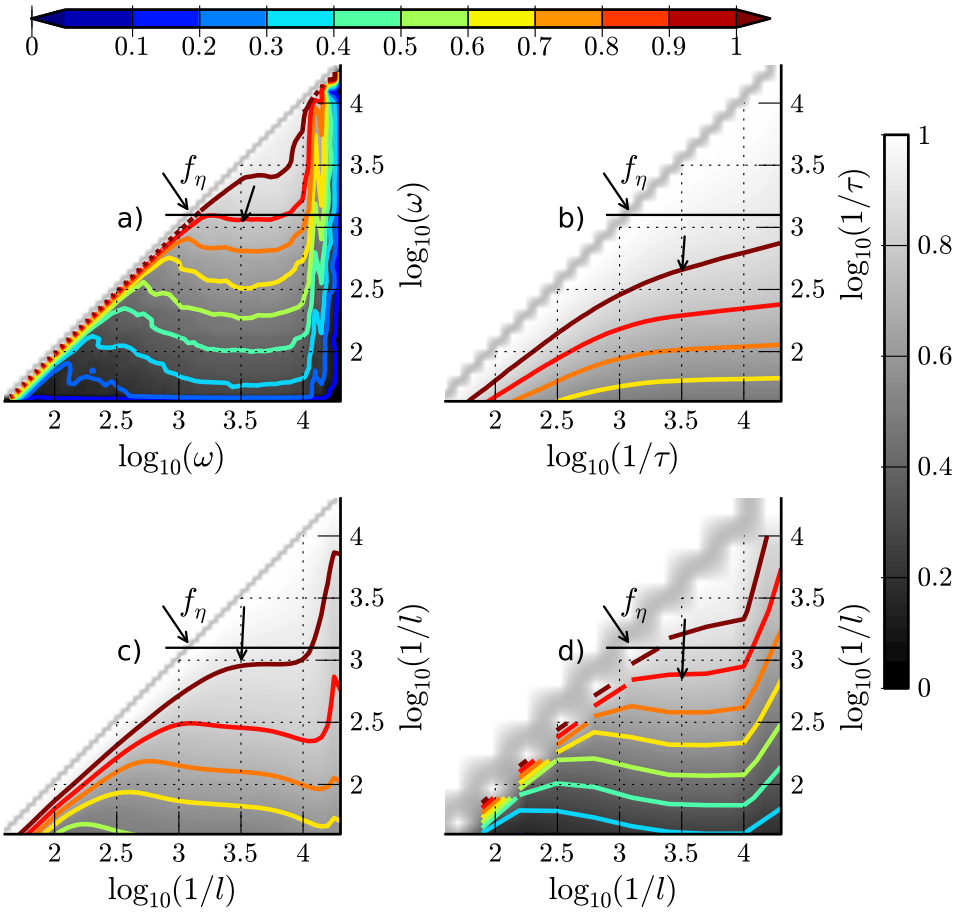

Figure 7. Contour plots of the measured TSC $\mathcal{R}$ for longitudinal velocity in a fully developed turbulent flow with a Taylor microscale based Reynolds number $Re_\lambda \simeq 720$: (a) Hilbert spectral analysis, (b) second-order SF, (c) continuous wavelet transform and (d) discrete wavelet transform with the db3 wavelet. The arrow indicates the contour line $\mathcal{R} = 0.8$. The Kolmogorov dissipation frequency f_η is indicated by a horizontal solid line.

motion transits from turbulent to laminar domains on these scales [16]. This is consistent with the Richardson–Kolmogorov energy cascade picture [20]. This can be regarded as evidence of nonlinear interactions for $0.2 < \mathcal{R} < 0.8$. It confirms that the Hilbert-based TSC analysis predicts not only a correct correlation trend but also correct details, e.g., the dissipation range and measurement noise. We would like to propose some comments on the choice of ΔT again here. As mentioned above, we have tested for different ΔT values in the range of 2^5–2^{14} data points. It is found experimentally that the correlation pattern is emerging when $\Delta T = 2^6$ and is stable when $\Delta T > 2^{12}$.

The contour line $\mathcal{R}$ = const. seems to be part of a circle. We therefore reproduce the contour line with several values of $\mathcal{R}$ from 0.3 to 0.7 in figure 8(b). The contour line is fitted by a circle with its center at $\omega_c \simeq 3200$ Hz, which is about 2.7 times the Kolmogorov dissipation frequency f_η. Note that we can divide the measured $\mathcal{R}$ into three different regimes. They are respectively the inertial–inertial regime, denoted as (1), the

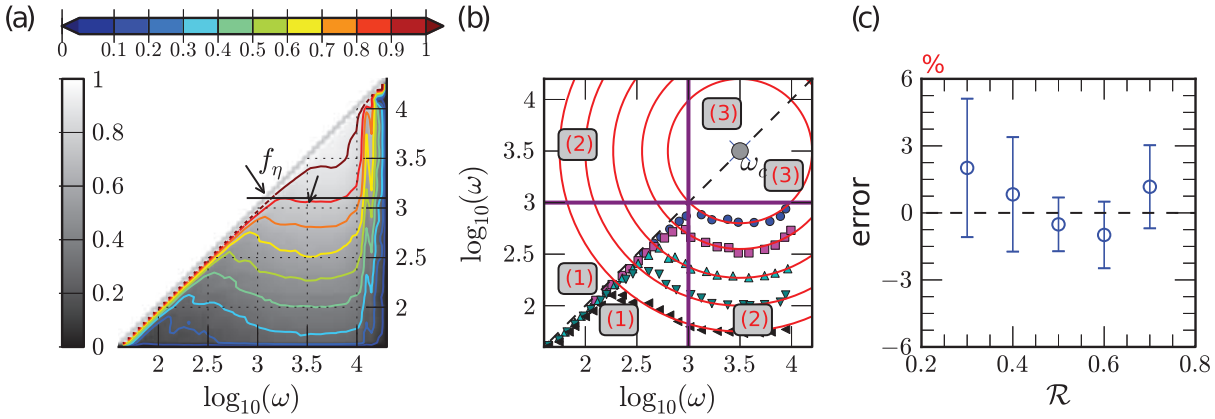

Figure 8. (a) Contour plot of the measured $\mathcal{R}$. (b) Replot of the contour lines with (from bottom to top) $\mathcal{R} = 0.3, 0.4, 0.5, 0.6, 0.7$ (symbols). The circle (solid line) is the fitting of the contour line with a circle centered at $\omega_c \simeq 3200$ Hz. Note that the measured $\mathcal{R}$ is divided into three regimes. They are respectively the inertial–inertial regime, denoted as (1), the inertial–dissipative regime, denoted as (2), and the dissipative–dissipative regime, denoted as (3). (c) The relative error between the fitted circle and the measured contour line. The error bar indicates the standard deviation for different contour lines.

inertial–dissipative regime, denoted as (2), and the dissipative–dissipative regime, denoted as (3). Figure 8(c) shows the measured relative error between the fitted circle and the corresponding contour line, in which the error bar indicates the standard deviation. The measured relative error is between -6% and 6%, showing a good approximation of the fitting circle. This implies that the correlation between two different scales is determined by the distance between the given scales (ω_i, ω_j) and the circle's center ω_c in the logarithmic frame. We thus represent in figure 9 the measured $\mathcal{R}$ with respect to $r = [(\log_{10}(\omega_i/\omega_c))^2 + (\log_{10}(\omega_j/\omega_c))^2]^{1/2}$, the radius of the fitted circle, for $\omega \leq 10^4$ Hz. The area $\omega > 1000$ Hz for dissipation–dissipation interaction is indicated by a quadrangle and denoted as (A). A log-law is observed in both the inertial and the dissipation ranges, which can be formulated as

$$\mathcal{R}(\omega_i, \omega_j) = -\alpha[(\log_{10}(\omega_i/\omega_c))^2 + (\log_{10}(\omega_j/\omega_c))^2]^{1/2}\,(1 - \delta_{i,j}) + \beta \qquad (8)$$

in which $\alpha = 0.37 \pm 0.01$ and $\beta = 1.01 \pm 0.02$ are obtained by using a least square fitting algorithm. If one considers the self-correlation, i.e., $\omega_i = \omega_j$, one has $\beta = 1$, which is consistent with the above measured β. The inset of figure 9 shows a compensated curve with the fitted parameters to emphasize the observed log-law. A large range of plateau is observed, confirming the log-law. We note that the observed log-law is valid not only in the dissipative–dissipative regime (illustrated by the dashed quadrangle in figure 9 and denoted as (A), see also (3) in figure 8(b)), but also in the inertial–inertial and inertial–dissipative regimes (denoted as (B) in figure 9, see also regimes (1) and (2) in figure 8(b)).

The measured α is coincidently the same as the scaling exponent $\zeta(1)$ of the first-order structure function for high Reynolds number turbulent flows [3, 30]. This logarithm law is

J. Stat. Mech. (2014) P05002

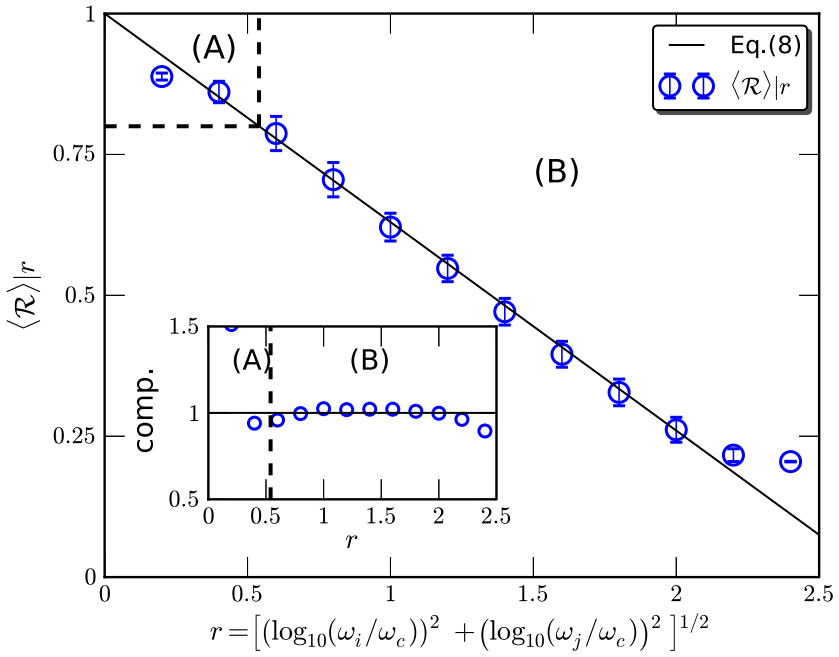

Figure 9. Representation of the measured $\mathcal{R}$ with respect to $r = [(\log_{10}(\omega_i/\omega_c))^2 + (\log_{10}(\omega_j/\omega_c))^2]^{1/2}$, the distance between the scale (ω_i, ω_j) and the circle's center ω_c in logarithmic coordinates, in which the error bar indicates the standard deviation of the measured $\mathcal{R}$ at given r. The dissipation range where $\mathcal{R} \geq 0.8$ and both ω_i and ω_j are larger than 1000 Hz is indicated by a dashed quadrangle and denoted as (A). A linear relation $\mathcal{R}(r) = \alpha r + \beta$ with $\alpha = -0.37 \pm 0.01$ and $\beta = 1.01 \pm 0.02$ is observed. The inset shows the compensated curve with fitted parameters $\alpha = 0.37$ and $\beta = 1$.

consistent with Kolmogorov's similarity hypotheses stating that the statistical quantities at small scales can be determined by the mean energy dissipation rate ϵ and the scale ω itself, since ω_c can be related to the Kolmogorov dissipation scale f_η [33, 38, 20]. However, the exact relation between the observed log-law and the Kolmogorov-like scaling exponent α with Kolmogorov's theory of turbulence is unclear. Moreover, it could be addressed by applying this method to more databases or different types of turbulent flow to see whether this log-law is validated.

We discuss here the nonlocal and nonlinear cascade/interaction indicated by our result. Note that the log-law correlation we observed here is valid over a broad range of scales: it is not only valid for the inertial–inertial scale, but also for the inertial–dissipative and dissipative–dissipative scales, see figure 8. Therefore, a nonlocal interaction/cascade is implied. The relative intensity of the interaction is characterized by the correlation coefficient, i.e., $\mathcal{R}(\omega_i, \omega_j)$. Statistical speaking, one can consider the measured $\mathcal{R}$ as a linear correlation when $\mathcal{R} \geq 0.8$, and as decoupling when $\mathcal{R} \leq 0.3$. Therefore, $\mathcal{R}$ can be regarded as experimental evidence of the nonlinear interactions when $0.3 < \mathcal{R} < 0.8$. This is related to the fluid viscosity partially through the central frequency ω_c, see equation (8), and partially through the inertial–dissipative interaction, see regime (2) in figure 8(b).

J. Stat. Mech. (2014) P05002

Finally, we want to make some comments on the recent work by Lalescu *et al* [34]. These authors performed pseudospectral simulation of the incompressible Navier–Stokes equations. They found that the so-called chaos synchronization theory can be used to interpret their observations in the numerical experiments, in which small-scale motions in the three-dimensional turbulent energy cascade could be subordinate to the chaotic dynamics of large-scale modes. Therefore, all sub-Kolmogorov length modes could be fully recovered from numerical simulations with a grid resolution of the standard Kolmogorov length [34]. Our observations here are consistent with their conclusion, showing that the small-scale motions above the averaged Kolmogorov scale are linearly correlated.

4. Conclusion

In summary, we propose in this paper a new approach to estimate the two-scale correlation in the frame of Hilbert spectral analysis. On applying this new approach to a longitudinal velocity obtained from fully developed turbulence, a logarithmic law is found in both the inertial and dissipation ranges with an exponent $\alpha = 0.37 \pm 0.01$. It can be considered as a self-similarity with respect to r, the distance between the given frequencies and a circle center ω_c. A triad-scale circle formula is proposed to describe this triadic nonlinear interaction, which is consistent with the classical Richardson–Kolmogorov energy cascade picture and indicates a nonlocal and nonlinear cascade. The origin of this log-law might be an effect of the fluid viscosity. This implies that the fluid viscosity is involved in the energy cascade process in which the viscosity is presented. Moreover, it is found that the Hilbert energy $E_H(\omega)$ satisfies a lognormal distribution. A power law behavior of the maximum pdf of the Hilbert energy in the logarithmic frame is observed experimentally with a scaling exponent of 0.33.

The Hilbert-based TSC analysis proposed here should certainly be applied to more databases to check whether the scaling exponent α we observed here is universal for other types of flow, e.g. shear flow, turbulent boundary layer, Rayleigh–Bénard convection system, etc. The Hilbert analysis we proposed here is general and applicable to other complex systems to check the relation between two scales, in the sense of energy or other statistical quantities; for example, the scale ω itself [23].

Acknowledgments

This work is sponsored by the National Natural Science Foundation of China under Grant Nos 11072139, 11032007, 11202122, 11272196 and 11332006, the ‘Pu Jiang’ project of Shanghai (No. 12PJ1403500) and the Shanghai Program for Innovative Research Teams in Universities. YH thanks Professor L Biferale for useful discussions and comments. We thank Professor C Meneveau for sharing his experimental velocity database, which is available for download at C Meneveau’s web page: www.me.jhu.edu/meneveau/datasets.html. The EMD MATLAB codes used in this paper were written by Dr Gabriel Rilling and Professor Patrick Flandrin from Laboratoire de Physique, CNRS & ENS Lyon (France): http://perso.ens-lyon.fr/patrick.flandrin/emd.html. We also thank the anonymous referees for their useful comments and suggestions.

References

[1] Alexakis A, Mininni P and Pouquet A, 2005 *Phys. Rev. Lett.* **95** 264503
[2] Arneodo A, Bacry E, Manneville S and Muzy J F, 1998 *Phys. Rev. Lett.* **80** 708
[3] Arneodo A, Baudet C, Belin F, Benzi R, Castaing B, Chabaud B, Chavarria R, Ciliberto S, Camussi R and Chilla F, 1996 *Europhys. Lett.* **34** 411
[4] Arneodo A, Manneville S, Muzy J and Roux S, 1999 *Phil. Trans. R. Soc.* A **357** 2415
[5] Baudet C, Michel O and Williams W, 1999 *Physica* D **128** 1
[6] Benzi R, Biferale L and Toschi F, 1998 *Phys. Rev. Lett.* **80** 3244
[7] Benzi R, Biferale L, Ruiz-Chavarria G, Ciliberto S and Toschi F, 1999 *Phys. Fluids* **11** 2215
[8] Burger K, Treib M, Westermann R, Werner S, Lalescu C, Szalay A, Meneveau C and Eyink G, 2012 arXiv:1210.3325
[9] Celani A, Musacchio S and Vincenzi D, 2010 *Phys. Rev. Lett.* **104** 184506
[10] Cencini M, Muratore-Ginanneschi P and Vulpiani A, 2011 *Phys. Rev. Lett.* **107** 174502
[11] Chevillard L, Mazellier N, Poulain C, Gagne Y and Baudet C, 2005 *Phys. Rev. Lett.* **95** 200203
[12] Cohen L, 1995 *Time–Frequency Analysis* (Englewood Cliffs, NJ: Prentice Hall PTR)
[13] Davidson P A and Pearson B R, 2005 *Phys. Rev. Lett.* **95** 214501
[14] Eyink G and Aluie H, 2009 *Phys. Fluids* **21** 115107
[15] Fairhall A, Dhruva B, L'vov V, Procaccia I and Sreenivasan K, 1997 *Phys. Rev. Lett.* **79** 3174
[16] Falkovich G, Xu H, Pumir A, Bodenschatz E, Biferale L, Boffetta G, Lanotte A S and Toschi F, 2012 *Phys. Fluids* **24** 055102
[17] Flandrin P, 1998 *Time–Frequency/Time-Scale Analysis* (New York: Academic)
[18] Flandrin P and Gonçalvès P, 2004 *Int. J. Wavelets, Multires. Info. Proc.* **2** 477
[19] Flandrin P, Rilling G and Gonçalvès P, 2004 *IEEE Signal Process. Lett.* **11** 112
[20] Frisch U, 1995 *Turbulence: The Legacy of AN Kolmogorov* (Cambridge: Cambridge University Press)
[21] Huang N E, Shen Z and Long S R, 1999 *Annu. Rev. Fluid Mech.* **31** 417
[22] Huang N E, Shen Z, Long S R, Wu M C, Shih H H, Zheng Q, Yen N, Tung C C and Liu H H, 1998 *Proc. R. Soc.* A **454** 903
[23] Huang Y, *Arbitrary-order Hilbert spectral analysis: definition and application to fully developed turbulence and environmental time series* 2009 *PhD Thesis* Université des Sciences et Technologies de Lille—Lille 1, France and Shanghai University, China
[24] Huang Y, Biferale L, Calzavarini E, Sun C and Toschi F, 2013 *Phys. Rev.* E **87** 041003(R)
[25] Huang Y, Schmitt F G, Gagne Y, Lu Z and Liu Y, 2011 *J. Phys.: Conf. Ser.* **318** 042003
[26] Huang Y, Schmitt F G, Hermand J P, Gagne Y, Lu Z and Liu Y, 2011 *Phys. Rev.* E **84** 016208
[27] Huang Y, Schmitt F G, Lu Z, Fougairolles P, Gagne Y and Liu Y, 2010 *Phys. Rev.* E **82** 026319
[28] Huang Y, Schmitt F G, Lu Z and Liu Y, 2008 *Europhys. Lett.* **84** 40010
[29] Huang Y, Schmitt F G, Lu Z and Liu Y, 2009 *J. Hydrol.* **373** 103
[30] Huang Y, Schmitt F G, Zhou Q, Qiu X, Shang X, Lu Z and Liu Y, 2011 *Phys. Fluids* **23** 125101
[31] Hutchins N and Marusic I, 2007 *Phil. Trans. R. Soc. A* **365** 647
[32] Kang H, Chester S and Meneveau C, 2003 *J. Fluid Mech.* **480** 129
[33] Kolmogorov A N, 1941 *Dokl. Akad. Nauk SSSR* **30** 301
[34] Lalescu C C, Meneveau C and Eyink G L, 2013 *Phys. Rev. Lett.* **110** 084102
[35] L'vov V and Procaccia I, 1996 *Phys. Rev. Lett.* **76** 2898
[36] Marusic I, Mathis R and Hutchins N, 2010 *Science* **329** 193
[37] Mathis R, Hutchins N and Marusic I, 2009 *J. Fluid Mech.* **628** 311
[38] Monin A S and Yaglom A M, 1971 *Statistical Fluid Mechanics vd II* (Cambridge, MA: MIT Press)
[39] Mouri H, Hori A and Takaoka M, 2009 *Phys. Fluids* **21** 065107
[40] Mouri H, Kubotani H, Fujitani T, Niino H and Takaoka M, 1999 *J. Fluid Mech.* **389** 229
[41] Pando J, Valls-Gabaud D and Fang L, 1998 *Phys. Rev. Lett.* **81** 4568
[42] Percival D and Walden A, 1993 *Spectral Analysis for Physical Applications: Multitaper and Conventional Univariate Techniques* (Cambridge: Cambridge University Press)
[43] Pope S B, 2000 *Turbulent Flows* (Cambridge: Cambridge University Press)
[44] Poulain C, Mazellier N, Chevillard L, Gagne Y and Baudet C, 2006 *Eur. Phys. J.* B **53** 219
[45] Tan H-S, Huang Y and Meng J-P, 2014 *Phys. Fluids* **26** 015106
[46] Rilling G, Flandrin P and Gonçalvès P, 2003 *IEEE-EURASIP Workshop on Nonlinear Signal and Image Processing (Grado, Italy)*
[47] Tsinober A, 2009 *An Informal Conceptual Introduction to Turbulence* (Berlin: Springer Verlag)
[48] Wood A and Chan G, 1994 *J. Comput. Graph. Stat.* **3** 409
[49] Wu Z-H and Huang N-E, 2004 *Proc. R. Soc.* A **460** 1597

J. Stat. Mech. (2014) P05002